Observation of dissociative recombination of Ne_2^+ and Ar_2^+ directly to the ground state of the product atoms

G. B. Ramos, M. Schlamkowitz, J. Sheldon, and K. A. Hardy
Florida International University, Miami, Florida 33199

J. R. Peterson
Molecular Physics Laboratory, SRI International, Menlo Park, California 94025

(Received 7 October 1994)

Using data gathered by the metastable atom time-of-flight technique, evidence is presented for the first time that some of the direct products of dissociative recombination (DR) in Ne_2^+ and Ar_2^+ are purely ground-state atoms. These results are very surprising because there are no evident curve crossings between the initial molecular-ion potentials and those of the repulsive ground states. Such curve crossings have been thought to be necessary for DR to occur. Using a laser-based atom beam deflection technique, it is shown that at least some of the fast ground-state atoms produced by DR are reexcited to metastable states that are easily detected.

PACS number(s): 34.50.−s

I. INTRODUCTION

It has long been commonly believed that dissociative recombination (DR) of free electrons with rare-gas dimer ions heavier than He_2^+, such as

$$e + Ar_2^+ \Longleftrightarrow (Ar_2^*)_{\text{unstable}} \rightarrow Ar^* + Ar + E_K \ , \qquad (1)$$

where E_K indicates the dissociative kinetic energy released to the atoms, yields one atom in the np^6 ground-state configuration and the other predominantly in the $np^5(n+1)p$ excited states [1]. This belief arose because optical (visible wavelength) measurements [2–4] showed that the $(n+1)p$ radiation to the $(n+1)s$ states dominated over similar radiation from other (higher) states. Also, it was generally thought [5] that direct population of the $(n+1)s$ states probably did not occur because the (repulsive) potential-energy curves leading to those Ar^*+Ar states passed inside (at smaller internuclear separations R) than the potentials of the Ar_2^+ ground state and thus the potentials did not intersect near the region of Ar_2^+ ($v=0$), as is required for a direct DR process [6,7]. However, it should be recognized that in those experiments, radiation from the $(n+1)s$ states was actually not observable; these states are either metastable or they radiate in the vacuum ultraviolet, which was not detected in those experiments. Furthermore, sufficiently reliable calculations have not been prepared to allow an accurate picture of the appropriate potentials.

Recently, however, we have found convincing evidence that in fact the $(n+1)s$ states actually dominate the excited products of all three species Ne_2^+, Ar_2^+, and Kr_2^+ [8,9], indicating that the older assumptions were incorrect. As a partial explanation (in addition to the lack of uv detection in the experiments), we note that in a recent study by Malinovsky *et al.* [10], which reported DR production of $3p$ and $3d$ states from Ne_2^+ using a traditional optical technique, the authors displayed calculated potential energy curves for Ne_2^+ and Ne_2^* that indicated a curve crossing by $3s$ repulsive states near the inner turning point of the Ne_2^+ ground vibrational state, which provides a mechanism for $3s$ production. A similar situation must occur in Ar_2^+ and Kr_2^+ even though it has not been shown.

We report here evidence that in some of the DR reactions involving Ne_2^+ and Ar_2^+ both atom products are completely in the ground state. This finding is totally surprising, as the repulsive ground-state potentials must lie well inside the inner turning points of the ionic ground state. We shall defer further discussion of these results until after they are presented.

The technique we have used to detect the metastable $(n+1)s$ products is also used here, and the data again reveal the importance of those states. Using a time-of flight (TOF) technique we are able to measure the kinetic energy E_K released in reaction (1). From it and the known values of the molecular-ion internal energies, and assuming that the initial kinetic energy is thermal (near 0 eV) as expected, we are able to deduce the values of the electronic energies of the final atomic states. This method is thus independent of any radiation subsequent to the dissociation.

II. APPARATUS

The molecular-beam apparatus used here is the same as the one used previously with some small changes [11]. The apparatus is shown in Fig. 1. The metastable atoms are generated in a continuous discharge source maintained by electrons produced by a directly heated thoria-coated tungsten ribbon (2.5×0.025 mm). The gas pressure was variable and ranged between 3 and 20 mTorr in this work. The discharge voltage ranged between 25 and 125 V. The data presented here were taken with a source pressure of approximately 8 mTorr for both neon and ar-

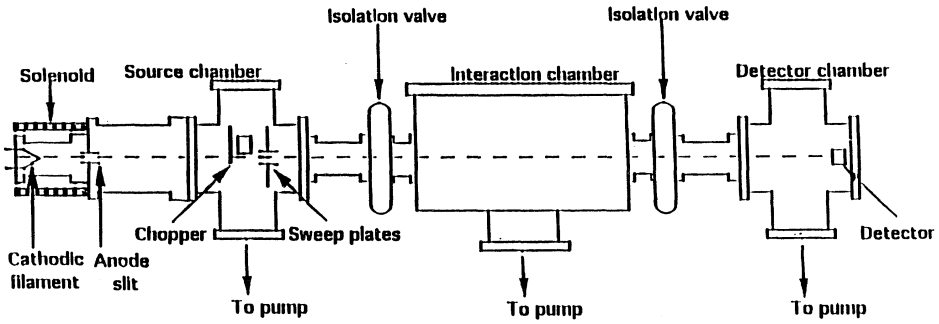

FIG. 1. Molecular-beam apparatus. The length of the flight path is 1.227 m. The laser radiation for the deflection experiments is introduced after the anode slit. The second beam-defining slit is located at the position of the chopper.

gon and discharge voltages of 100 V for neon and 52 V for argon. The source is surrounded by a solenoid that produces a variable axial magnetic field of up to 225 G; it is normally operated at about 175 G [11]. This field was found to increase the ratio of fast metastable atoms to thermal metastable atoms by at least 10 times the ratio found with no magnetic field.

Within the discharge, the high-energy electrons with energies approximately equal to the discharge voltage in eV create both excited states of atoms and atomic ions. Excited states are also produced by secondary electrons following primary collisions. At the pressures used here, molecular ions are formed principally by associative ionization

$$Ar^* + Ar \rightarrow Ar_2^+ + e \ ,$$

where Ar* is in a sufficiently high Rydberg state ($n > 5$). Subsequently, slow electrons dissociatively recombine with molecular ions to form fast neutral products. The effect of the axial magnetic field is to constrain the discharge, by constricting both fast and slow electrons to a narrow region along the axis, in alignment with the filament and the exit slit of the discharge. Thus excitation, ionization, and DR all occur close to the axis, which increases the observed yield of fast metastable states so effectively.

The exit slit for the source is 6.35×0.5 mm^2 and produces a vertical ribbon beam which is defined by a second 6.35×0.5 mm^2 slit 46.3 cm downstream from the source. The angular spread of the beam is thus 2.2×10^{-4} rad. The chopper wheel slits give an open time of 86 μs. The flight path passes through three vacuum chambers where the vacuum is maintained at about 1×10^{-7} Torr. Sweep plates located at the second set of beam-defining slits maintain an electric field of about 250 V/cm, which removes all charged particles and long-lived Rydberg states. The detector entrance slit, which is 6.35×0.1 mm^2, passes the particles in the beam to a tungsten catcher plate from which electrons are ejected by the Auger effect. The electrons are collected and detected by a Channeltron electron multiplier. The data are processed with an Ortec multichannel scalar card and software operating in a Zenith personal computer. The channel width used in these experiments is 40 μs and the sweep length is 90 channels to allow the detection of the slow tail of the Maxwellian velocity distribution of metastable atoms from the discharge.

III. EXPERIMENTAL RESULTS

In the following discussion it is assumed that one of the DR products is always in the ground state. We will consider only the nascent states of the other product atom. All deduced relations are based on this model. Typical time distributions for neon and argon are shown in Figs. 2(a) and 2(b). The most prominent features in these dis-

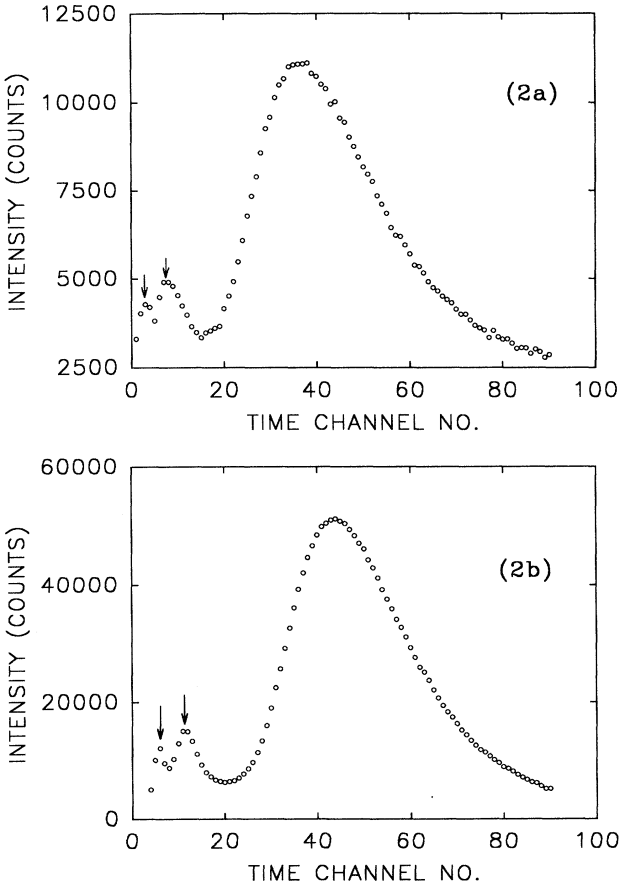

FIG. 2. TOF distributions for (a) neon and (b) argon. Distributions showing DR reaction products to the s states and to the ground state. The typical Maxwellian TOF distribution is also shown. The time channel width is 40 μ/s in both cases with $t = 0$ at channel 0. The arrow indicate the ground state and the $3s$ state (neon) or $4s$ state (argon).

tributions are the broad Maxwellian distributions with most probable velocities of approximately 875 m/s for neon and 700 m/s for argon. These velocities both correspond to an approximate temperature of 1000 K, which is characteristic of the metastable atoms in the discharge region. At shorter arrival times, below channel 20, are the smaller superthermal fast atom peaks that result from dissociative recombination. Actually these peaks can be grouped into a "fast" peak representing DR to an excited state and a smaller "superfast" component, which we did not distinguish earlier [11] and which we now identify with purely ground-state products. These peaks can be seen clearly in the short arrival time data of Fig. 3.

Knowing the ionization energy of the rare-gas atom E_i, the dissociation energy of the molecular ion D_0, and the energy of the final states $E_{\rm FS}$, the dissociative kinetic energy E_K can be calculated using

$$E_K = E_i - D_0 - E_{\rm FS} \ . \tag{2}$$

Since we are dealing with homonuclear systems, the energy of the individual atoms E_d is equal to one-half of E_K. The ionization energies E_i are 21.56 and 15.76 eV for neon and argon, respectively [12]. The binding energies of the molecular ion D_0 are less well known. We used 1.27 ± 0.02 eV [13] for neon and 1.26 ± 0.03 eV [14] for argon. The energies and corresponding velocities for the superfast peaks are 10.08 and 7.21 eV, which correspond to velocities of 9823 and 5906 m/s for neon and argon, respectively. These are the velocities expected from the DR reaction directly to the ground state. The velocities of the fast peaks are 4172 and 2661 m/s for neon and argon, respectively. The neon fast peak velocities agree with the velocity computed from a $(2J+1)$ weighted average of the velocities for DR to the $3s\,[5/2]\ J=2$ and the $3s'[1/2]\ J=0$ metastable final product states. In argon, these are the $4s$ and $4s'$ states. The weighting factors used were the statistical weights of 5:1 expected for the metastable-state populations of 5 to 1. The corresponding energies of these products are 1.71 and 1.66 eV for the $J=2$ and 0 states in neon and 1.49 and 1.40 eV for the $J=2$ and 0 states in argon.

IV. ANALYSIS OF THE DATA

The velocity of a DR product in the laboratory system v_L is the sum of the c.m. thermal velocity given by the Maxwellian velocity distribution characterized by a most probable velocity v_p and the randomly directed velocity $v_{\rm DR}$ of the product in the c.m. system. Thus the peak due to DR to a single final state is broadened by the Boltzmann distribution on the ions. The DR atom flux dJ from the source discharge within a laboratory angle $\Delta\theta_L$ about $\theta_L=0$ is given by

$$dJ = \frac{n}{4\pi^{5/2}v_p^3}\int_{\theta_L=0}^{\Delta\theta_L}\int_{\phi_L=0}^{2\pi}\int_{\theta_{\rm DR}=0}^{\pi}\int_{\phi_{\rm DR}=0}^{2\pi} v_L\cos\theta_L \exp[-(U_x^2+U_y^2+U_z^2)]\sin\theta_{\rm DR}\,d\theta_{\rm DR}\,d\phi_{\rm DR}\sin\theta_L\,d\theta_L\,d\phi_L\,v_l^2\,dv_L \ , \tag{3}$$

where

$$U_x = (v_L\sin\theta_L\cos\phi_L - v_{\rm DR}\sin\theta_{\rm DR}\cos\phi_{\rm DR})/v_p \ ,$$

$$U_y = (v_L\sin\theta_L\sin\phi_L - v_{\rm DR}\sin\theta_{\rm DR}\sin\phi_{\rm DR})/v_p \ ,$$

and

$$U_z = (v_L\cos\theta_L - v_{\rm DR}\cos\theta_{\rm DR})/v_p \ .$$

For small angles $\Delta\theta_L$, this distribution reduces to

$$dJ \simeq \frac{nv_p\Delta\theta_L^2 v_L^2}{2\pi^{1/2}v_{\rm DR}}\exp\left[-\frac{(v_L-v_{\rm DR})^2}{v_p^2}\right]dv_L \ , \tag{4}$$

which, when converted to the TOF distribution, becomes

$$dJ(t) = \frac{C}{t^4}\exp\left[-\left[\frac{(L/t)-v_{\rm DR}}{v_p}\right]^2\right]dt \ , \tag{5}$$

where C is an arbitrary constant, L is the length of the flight path, and t is the TOF. The velocities expected $V_{\rm DR}$ can be found from Eq. (2) for the DR reaction to a specific state in the product atom. DR occurs primarily with low-energy electrons [7] so the electron energy is assumed to be near zero.

Figures 3(a)–3(c) are expanded plots of the fast arrival time distributions showing the data and fits to the data using Eq. (5). The only free parameters in the fits are the background, the amplitude of the peaks, and T_0, the time at which the chopper is open. It can be seen that the positions of the peaks agree well with those expected for the products of the DR reaction to the ground state and the metastable states. We have found that in DR to the $3s$ (in neon) and $4s$ (in argon) states, the widths of the DR lines agree with the widths v_p characteristic of the Maxwellian velocity distribution. The widths of the ground-state peaks are somewhat wider than the widths v_p characteristic of the Maxwellian velocity distribution. The peak in the data near channel 3 shown in Fig. 3(a) illustrates the DR reaction to the ground state in neon. The data were fitted using three lines with velocities of 9823, 4172, and 2880 m/s. These velocities correspond to DR directly to the ground state, to the combined $3s\,[3/2]\ J=2$ and the $3s'[1/2]\ J=0$ states and to the $3p[5/2,3/2]\ J=3,2,1,2$ states. As mentioned earlier, the velocity used for the $3s$ state is a weighted average of the velocities expected for the metastable states. The data in the figure show peaks that have areas with ratios of 0.014, 0.043, and 0.005 for the ground $3s$ and $3p$ states compared to the area of the thermal distribution. The data shown are sums of data taken with a variety of source conditions where the discharge voltage ranged from 85 to 120 V and the discharge pressure ranged between 13 and 28 mTorr. They indicate that under some source conditions a substantial fraction of the DR reactions proceed directly to the ground state of both atoms.

The data shown in Fig. 3(b) illustrate the DR reaction

to the ground state in argon. The data were fitted using two lines with velocities of 5907 and 2661 m/s, which respectively correspond to DR reactions directly to the ground state and to the combined $4s[3/2]\ J=2$ and $4s'[1/2]\ J=0$ metastable states. Again, the velocity is the weighted average of the velocities for the two combined states. This weighting gives satisfactory fits and we hope, in further studies, to determine the actual mix of metastable states in the fast peak. The data in the figure show peaks with area ratios of 0.035:1 for the ground state and 0.065:1 for the $4s$ states, compared to the area of the thermal distribution. There was no noticeable contribution from the $4p$ states in the case of argon for the source conditions used in the data shown in Fig. 3, although small ($\approx 10\%$ of the $4s$ states) $4p$ contributions were found in our previous work. The source conditions used for the argon data shown were a pressure of 14 mTorr, a discharge voltage of 52 V, and a magnetic induction of 120 G [9].

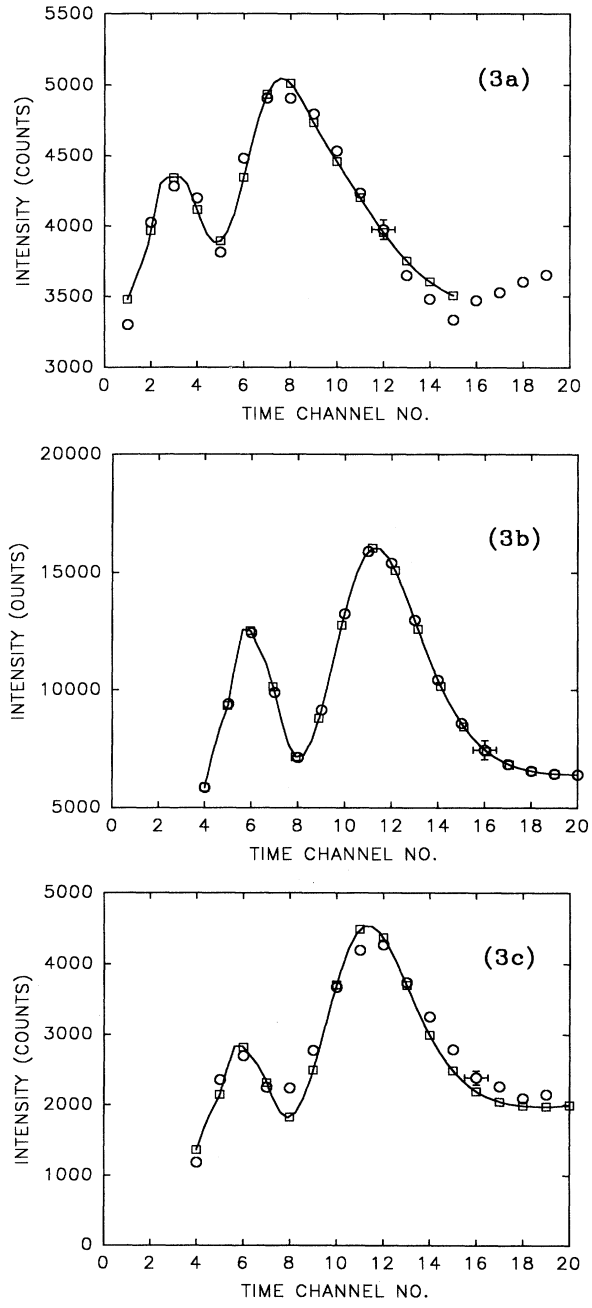

FIG. 3. Expanded TOF distributions for (a) neon, (b) argon, and (c) the laser on-off difference time distribution for argon. The time interval in all cases is 40 μ/s per channel with the $t=0$ at channel 0. The circles are the data points, the squares are the fit to the data. A line through the fit points is drawn to guide the eye. In all cases the only free parameters were the amplitude of the peaks and not their position.

V. METASTABLE-STATE IDENTIFICATION BY LASER DEFLECTION

Although the arrival times of the superfast peaks in both Ne and Ar just match the expected velocities expected from purely ground-state products, which is a surprising result, it is also surprising that these atoms are even detected in our apparatus. Certainly the kinetic energy of the ground-state product of the DR reaction (10.0 and 7.3 eV for neon and argon, respectively) is slightly above the work function of the tungsten catcher plate (4.5 eV), but there is no report in the literature [15] of neutral atoms in this velocity range being detected with a detector of our design which normally depends on the Auger effect for the metastable states to eject electrons from a catcher plate. Since the sweep plates remove charged particles and high Rydberg state atoms from the atom beam, the only species to reach the detector are neutral metastable or ground-state atoms. If the ground-state products of DR were somehow reexcited to a metastable state in the source, they would be easily detectable. To examine this possibility, we have used a laser-induced deflection technique which is sensitive only to metastable argon atoms. For this study, the flight path has been lengthened to 122.7 cm and the beam-defining slits have been narrowed to give better angular definition to the beam for metastable-state separation measurements. The metastable states are separated by deflecting the $J=2$ metastable state with the force due to the resonant absorption of laser radiation. Windows have been added at two locations in the beam path to allow the introduction of laser radiation perpendicular to the beam path.

The $J=2$ metastable state component of the atom beam was deflected by passing laser radiation perpendicular to the atom beam resonant to the $4s[3/2]\ J=2 \rightarrow 4p[5/2]\ J=3$ transition in argon. This transition forms a closed system as the $J=3$ state can only decay to the $J=2$ state and because the lifetime of the $J=2$ metastable state is much longer than the TOF in our experiment. The laser radiation was derived from a grating-stabilized diode laser tuned to the saturated absorption line in an argon discharge. The design of the laser is similar to that described by MacAdam, Steinbach, and Wieman [16]. The wavelength of the transition is 811.73 nm and our laser system yields approximately 15 mW with a long-term stabilized linewidth of approximately 30 MHz. A quarter wave plate was used to con-

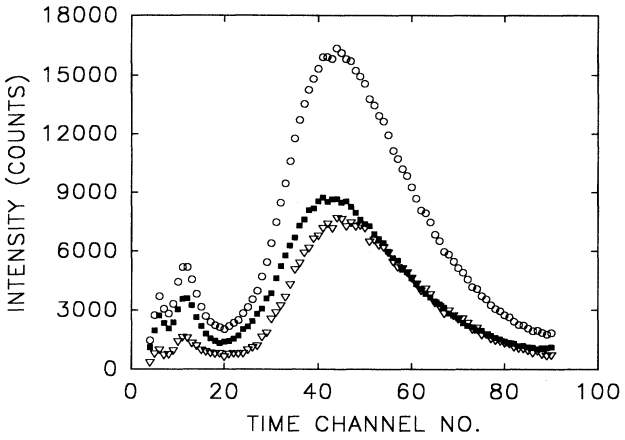

FIG. 4. TOF distribution for argon. The figure shows a TOF distribution with the deflecting laser off (circles), the deflecting laser on (squares), and the difference between the two (triangles). Since only the $4s$ $J=2$ state in argon is deflected, the difference spectrum represents a pure $4s$ $J=2$ time distribution. Note the deflection of the ground-state peak.

vert the linear polarized radiation from the laser diode to σ^+ radiation. The laser radiation was chopped at 0.5 Hz to compensate for any small variations in atom beam intensity.

Figure 4 shows three arrival time spectra taken with the laser on, the laser off, and the difference between the two. In our apparatus, we have deflected about 70% of the thermal metastable atom beam compared to the statistically expected deflection of 83% of the beam. The difference between the laser on and off spectra yields a pure $4s[3/2]$ $J=2$ metastable atom spectrum. The data in Fig. 3(c) show the difference between laser-on and laser-off time distributions for argon. Since only the $4s[3/2]$ $J=2$ metastable state is deflected, these difference data represent a time spectrum for the $4s[3/2]J=2$ metastable state only and the data clearly show the ground-state peak at 5907 m/s. Because our detectors are designed specifically to detect thermal metastable states, these deflection data should resolve any question concerning the mechanism of detection of at least some of the super fast products.

VI. CONCLUSION

We conclude from these results that some of the DR events in our apparatus produce both atoms in the ground state and that among those superfast DR products, some, perhaps many, are reexcited into metastable $J=2$ states. Such reexcitation could occur either by electron impact or by electron exchange with thermal metastables. Preliminary estimates show that neither process seems likely, but whatever process occurs probably takes place within the narrow discharge region. Estimates of the metastable densities based on the arrival rates at the detector and its subtended solid angle are insufficient for the exchange process, so we conclude that the effective mechanism must involve those primary and secondary electrons within the discharge whose energies are sufficient for the excitation, which includes cascading from higher states [17,18]. The magnetic field certainly aids this process by confining the electrons. We can also consider the possibility of direct detection of ground-state DR products. Although the efficiencies of kinetic ejection of secondary electrons by neon atoms of 10 eV and argon atoms of 7.3 eV are not known, they are probably small but nonzero. These metastable atom deflection data do not rule out that possibility, but they certainly explain the detectability of at least some of the ground-state DR products.

Further studies are certainly warranted, but the observation of a superfast peak whose velocities correspond to ground-state DR seems convincing and we can envision no alternative source other than DR. We have considered the possibility of artifacts, but without success.

Although the finding of some DR to ground-state channels is very surprising, there is some rationale for its occurrence. For instance, dissociative recombination in the absence of a curve crossing was once considered negligible, but it has very recently been found by Guberman to explain experimental results in the case of HeH^+ [19], where the process yields primarily $n=2$ states. We have already found [8,9] that in Ne_2^+, Ar_2^+, and Kr_2^+ the excited products are dominated by $(n+1)s$ states which were previously *not* expected because of the supposed lack of appropriate curve crossings. A similar effect as in HeH^+ must also occur here for the primary $(n+1)s$ channels and also for the more weakly coupled ground states. We are aware of no actual theoretical work on the DR of Ne_2^+ of Ar_2^+. Most calculations of the potential-energy curves of the excited neutral dimers have been aimed toward interpreting the observed optical spectra from afterglows or laser-induced transitions and little attention has been given to other aspects relevant to DR, with the recent exception of Malinovsky *et al.*, whose work focused on the DR production of Ne $(3p)$ and Ne $(3d)$ states [10]. As mentioned earlier, the Ne_2^+ and Ne_2^* potentials shown in the latter work indicate the possibility of DR to the Ne $(3s)$ states, which were not discussed. It is hoped that our present and earlier results [8,9] will stimulate some theoretical efforts to understand both the dominance of the $(n+1)s$ state and the ground-state channels. It would be interesting to examine the relative production of ground-state and excited channels by some method that is independent of the internal energy in the products, such as translational spectroscopy carried out on DR products using the technique of a merged electron beam plus storage ring experiment at high ion-beam energies.

ACKNOWLEDGMENTS

One of the authors (K.H.) would like to thank H. Metcalf of SUNYS and W. Phillips of NIST for many helpful discussions about the laser deflection experiments. K.H. and J.W. received partial support from AFOSR Grant No. F49620-89-K-0002 and J.P. received partial support from NSF Grant No. PHY 9111872.

[1] D. F. Heustis, in *Applied Atomic Collision Physics, VIII Gas Lasers,* edited by E. W. Mcdaniel and W. L. Nighan (Academic, New York, 1982); M. A. Biondi, *ibid.*
[2] L. Frommhold and M. A. Biondi, Phys. Rev. **185**, 244 (1969).
[3] Y. J. Shiu and M. A. Biondi, Phys. Rev. A **16**, 1817 (1977).
[4] Y. J. Shiu and M. A. Biondi, Phys. Rev. A **17**, 868 (1978).
[5] D. C. Lorents, Physica C **82**, 19 (1976).
[6] J. N. Bardsley, J. Phys. B **1**, 365 (1968).
[7] F. J. Mehr and M. A. Biondi, Phys. Rev. **176**, 322 (1968).
[8] A. Barrios, J. W. Sheldon, K. A. Hardy, and J. R. Peterson, Phys. Rev. Lett. **69**, 1348 (1992).
[9] J. R. Peterson, in *Dissociative Recombination,* edited by B. R. Rowe, J. B. A. Mitchell, and A. Canosa (Plenum, New York, 1993), p. 263.
[10] L. Malinovsky, P. Lukáč, J. Trnovec, C. J. Hong, and A. Tálsky, Czech. J. Phys. **40**, 191 (1990).
[11] A. Barrios, G. B. Ramos, K. A. Hardy, and J. W. Sheldon, J. Appl. Phys. **76**, 728 (1994).
[12] C. E. Moore, *Atomic Energy Levels,* Natl. Bur. Stand. (U.S.) Circ. No. 467 (U.S. GPO, Washington, DC, 1949).
[13] K. P. Huber and G. Herzberg, in *Molecular Spectra and Molecular Structure IV, Constant of Diatomic Molecules* (Van Nostrand Reinhold, New York, 1979), give $D_e = 1.30$ eV and $\omega_e = 510\ \mathrm{cm}^{-1}$ for Ne_2^+.
[14] P. M. Dehmer and S. T. Pratt, J. Chem. Phys. **76**, 843 (1982).
[15] See R. D. Rundel, F. B. Dunning, J. S. Howard, J. P. Riola, and R. F. Stebbings, Rev. Sci. Instrum. **44**, 60 (1973); and F. B. Dunning, R. D. Rundel, and R. F. Stebbins, *ibid.* **46**, 697 (1975).
[16] K. B. MacAdam, A. Steinbach, and C. Wieman, Am. J. Phys. **60**, 1098 (1992).
[17] A. A. Mityureva and V. V. Smirov, J. Phys. B **27**, 1869 (1994).
[18] R. S. Schappe, M. B. Schulman, L. W. Anderson, and C. C. Lin, Phys. Rev. A **50**, 444 (1994).
[19] S. L. Guberman, Phys. Rev. A **49**, R4227 (1994).